

Rethinking Model Redundancy for Low-light Image Enhancement

Tong Li¹ Lizhi Wang^{2*} Hansen Feng¹ Lin Zhu¹ Wanxuan Lu³ Hua Huang²
¹Beijing Institute of Technology ²Beijing Normal University ³Chinese Academy of Sciences

Abstract

Low-light image enhancement (LLIE) is a fundamental task in computational photography, aiming to improve illumination, reduce noise, and enhance the image quality of low-light images. While recent advancements primarily focus on customizing complex neural network models, we have observed significant redundancy in these models, limiting further performance improvement. In this paper, we investigate and rethink the model redundancy for LLIE, identifying parameter harmfulness and parameter uselessness. Inspired by the rethinking, we propose two innovative techniques to mitigate model redundancy while improving the LLIE performance: Attention Dynamic Reallocation (ADR) and Parameter Orthogonal Generation (POG). ADR dynamically reallocates appropriate attention based on original attention, thereby mitigating parameter harmfulness. POG learns orthogonal basis embeddings of parameters and prevents degradation to static parameters, thereby mitigating parameter uselessness. Experiments validate the effectiveness of our techniques. We will release the code to the public.

1. Introduction

Low-light image enhancement (LLIE) aims to improve illumination, reduce noise, and enhance image quality of the low-light images [74], which is a fundamental task in computational photography [38] and an essential step for high-level computer vision tasks [43, 44]. The diverse degradation impose significant challenges for LLIE methods [78, 85]. Achieving high-quality results with suitable color and brightness has been a longstanding objective in this field [30, 76].

The mainstream approaches train neural network models to map low-light images to high-light images [5, 38]. In recent years, most research efforts focused on customizing complex neural network models, evolving from CNN-based models [32, 78], Transformer-based models [5, 84], to Mamba-based models [2, 17].

*Corresponding Author: Lizhi Wang (wanglizhi@bnu.edu.cn)

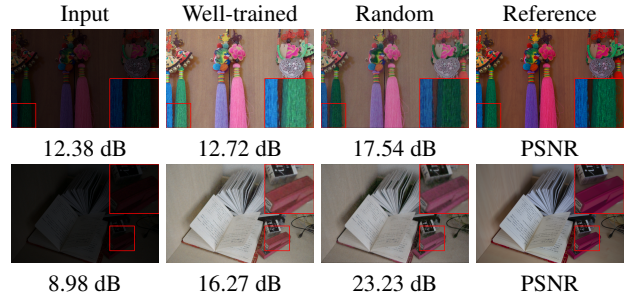


Figure 1. **We observe significant redundancy in low-light image enhancement models.** From left to right, the images are as follows: the low-light image, the image enhanced by the original well-trained Restormer [84], the image enhanced by the Restormer in which certain attention mechanism parameters have been reset to random values, and the reference image. The image enhanced with the well-trained parameters exhibits overexposure and fading color, with only 12.72 dB. In contrast, the images enhanced with random parameters show even higher PSNR values, along with more accurate color and brightness. This phenomenon suggests that there is significant model redundancy, as some parameters are useless or harmful.

However, we have observed significant redundancy in existing models, particularly in the attention mechanism [61]. Surprisingly, resetting specific parameters to random values even improves the enhancement performance for some images, as illustrated in Figure 1. This observation underscores the overlooked model redundancy, which prevents the model from fully utilizing the enhancement capacity, posing a substantial barrier against further performance improvement [8, 54].

Currently, limited research has considered model redundancy in LLIE. In other tasks, such as video object detection [12] and neural machine translation [62], FLOPs and accuracy are used to detect model redundancy. Methods to mitigate model redundancy typically involve network pruning [20, 22, 45], parameter quantization [4, 19, 50], and model distillation [1, 23]. However, these methods primarily aim to accelerate computation through techniques such as cutting removable neurons or channels, but inevitably trade off the performance.

In this paper, we rethink the model redundancy for LLIE,

which establishes the foundation to mitigate model redundancy while improving LLIE performance. Our investigation stems from resetting parameters to random values to detect redundancy, which yields insightful observations about the nature of model redundancy. Inspired by these observations, we rethink the manifestations and the reasons for model redundancy, identifying parameter harmfulness and parameter uselessness. To mitigate model redundancy, we propose two key techniques: Attention Dynamic Reallocation (ADR) and Parameter Orthogonal Generation (POG).

The underlying reason for parameter harmfulness lies in the parameter sharing mechanism. Current LLIE models apply static parameters learned after training to all input images, disregarding differences in image content. This parameter sharing mechanism treats all images equally [79], resulting in harmful parameters for some images. Inspired by the human brain theory about attention allocation and error processing [6, 7, 42, 57], we introduce an attention dynamic reallocation (ADR) technique. ADR dynamically reallocates appropriate attention based on original attention to deal with preceding errors, effectively alleviating parameter harmfulness.

The underlying reason for parameter uselessness lies in the dynamic parameter degradation. The current dynamic parameter mechanism learns multiple candidate parameters and dynamically weights candidate parameters based on input. However, the similarity and correlation in the candidate parameters lead dynamic parameters to degrade to static parameters, rendering all candidate parameters useless. Inspired by matrix analysis theory [25, 47], we propose a parameter orthogonal generation (POG) technique. POG learns orthogonal basis embeddings of parameters and dynamically generates suitable parameters based on the orthogonal bases, preventing degradation to static parameters and alleviating parameter uselessness.

Our contributions are summarized as follows:

- We rethink the model redundancy for LLIE, identifying parameter harmfulness and parameter uselessness.
- We propose an attention dynamic reallocation (ADR) technique, to mitigate the parameter harmfulness.
- We propose a parameter orthogonal generation (POG) technique, to mitigate the parameter uselessness.
- Experiments show our techniques mitigate model redundancy while improving the performance of LLIE.

2. Related work

2.1. Low-light image enhancement

Traditional low-light image enhancement methods focus on employing image priors, for example, histogram equalization [52], gama correction [71] and Retinex theory [34, 35]. Histogram-based methods [11, 51–53] and gamma-based methods [28, 71] focus on directly enhancing illumination.

These methods typically rely on empirically derived prior knowledge to achieve brightness adjustments. Retinex-based methods [18, 34, 35, 41, 65] are grounded in human cognition theories, dividing the image into an illumination map and a reflectance map. These Retinex-based methods generally require enhancing the illumination map while simultaneously denoising the reflectance map. However, the ability of these traditional methods in complex degradation conditions is limited.

With the development of deep learning, learning-based methods become the mainstream methods. Current mainstream approaches train neural networks to map low-light images to high-light images [43, 44]. In recent years, most research efforts focused on refining the neural network architectures [2, 5, 70, 83, 84]. The low-light image enhancement methods have evolved from CNN-based methods [32, 39, 49, 58, 64, 67, 74, 87, 88] to Transformer-based methods [66, 77, 83, 84], Diffusion-based methods [26, 30, 82, 90] and Mamba-based methods [2, 17, 75, 86]. As networks become more advanced, the enhancement performance improves. However, the significant model redundancy within these methods prevents further performance improvement.

2.2. Model redundancy

Model redundancy in static parameters has been observed by various methods [9, 29, 45, 72], but research on model redundancy in dynamic convolution remains scarce.

Existing researches usually attribute model redundancy to the presence of removable neurons, features, channels or blocks, which aim to accelerate computation and achieve a similar or competitive performance [33, 40]. Thus FLOPs, accuracy and precision are used to detect model redundancy [31, 81]. Some initial research focuses on reducing model redundancy during training by decomposing the weight and learning low-rank weights [27, 54]. More research targets reducing model redundancy post-training through techniques such as network pruning [20–22, 45, 48], parameter quantization [4, 19, 50], and model distillation [1, 23]. For instance, recent methods like [13, 72] prune related weights using graph theory, while [12, 81] reuse intermediate computations to eliminate temporal redundancy and improve efficiency.

However, limited research has considered model redundancy of low-light image enhancement, leading to a divergence in objectives. Existing methods simply accelerate computation, but inevitably trade off the performance.

3. Rethinking

As previous researches neglect LLIE, to find solutions for mitigating model redundancy while improving performance, we investigate and rethink the model redundancy for LLIE.

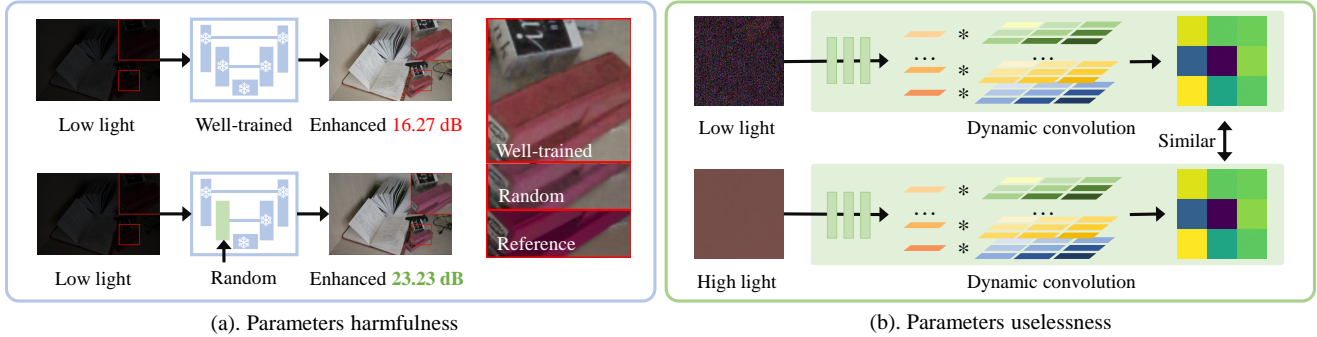


Figure 2. **Model redundancy manifests as parameter harmfulness and uselessness.** Harmfulness: Random parameters can yield better results than the well-trained parameters for some images. Uselessness: The existing dynamic mechanism (dynamic convolution) tends to generate similar parameters for different images, thus the parameters in the dynamic mechanism become useless.

Table 1. The first observation is that attention layers exhibit greater model redundancy than feedforward layers in transformer architectures.

Reset Parameters	All-layers	Latent-layers
Attention	- 5.52 dB	+ 0.02 dB
FeedForward	- 6.58 dB	+ 0.02 dB

Table 2. The second observation is that static parameters exhibit greater model redundancy than dynamic parameters. NOL represents the number of layer parameters to be reset to random ones.

NOL	1st	2nd	3rd	4th	5th	6th
Static	- 1.72	+ 0.05	+ 0.30	- 0.99	- 0.01	+ 0.01
Dynamic	-3.39	-1.55	-0.44	-2.65	-0.16	-0.01

Table 3. The third observation is that certain parameters are harmful. POI represents the percentage of images that get better results when replacing the well-trained parameters with the random ones.

NOL	1st	2nd	3rd	4th	5th	6th
POI	40%	33%	33%	27%	27%	33%

3.1. Investigation

To detect model redundancy in parameters, we reset the well-trained parameters of Restormer [84] to random values and then evaluate the LLIE performance. We examine two types of parameters: static parameters and dynamic parameters. Static parameters refer to the standard convolution layers, while dynamic parameters are generated by dynamic convolution [10]. The dynamic convolution learns multiple candidate parameters and weights candidate parameters based on the input image characteristics.

There are several intriguing observations and findings.

1. The first observation is that attention layers exhibit greater model redundancy than feedforward layers in transformer architectures. Resetting all attention layers caused

a smaller performance drop than resetting all feedforward layers, as shown in Table 1, indicating that there is more redundancy within the attention layers.

2. The second observation is that static parameters exhibit greater model redundancy than dynamic parameters. Resetting static parameters caused a smaller performance drop than resetting dynamic parameters, as shown in Table 2, indicating that there is more redundancy within static parameters.

3. The third observation is that certain parameters harm the performance. Resetting the attention parameters sometimes even improves PSNR as shown in Table 1, Table 2 and Table 3. These results suggest that there is redundancy in the model, with some well-trained parameters potentially even harming performance.

The first observation guides us in exploring model redundancy within attention mechanisms. The second observation suggests that dynamic parameters can help mitigate model redundancy. However, an alternative method for generating dynamic parameters may be necessary, as current dynamic convolution still exhibits model redundancy. The third observation indicates that static parameters harmfully impact certain images. These observations inspire us to further rethink and investigate the manifestations and underlying reasons for model redundancy. Here, we believe model redundancy manifests as parameter harmfulness for static parameters and parameter uselessness for dynamic parameters, respectively, as shown in Figure 2. The rethinking, along with relevant validated experiments and analyses, is presented below.

Harmfulness. Model redundancy in static parameters arises because some parameters are harmful at the individual image level. Our experiments verify that well-trained parameters can sometimes perform worse than random parameters for certain images. For instance, resetting the parameters of a single layer leads to better results for around 30% images as shown in Table 3, even improve 0.3dB PSNR as shown in Table 2.

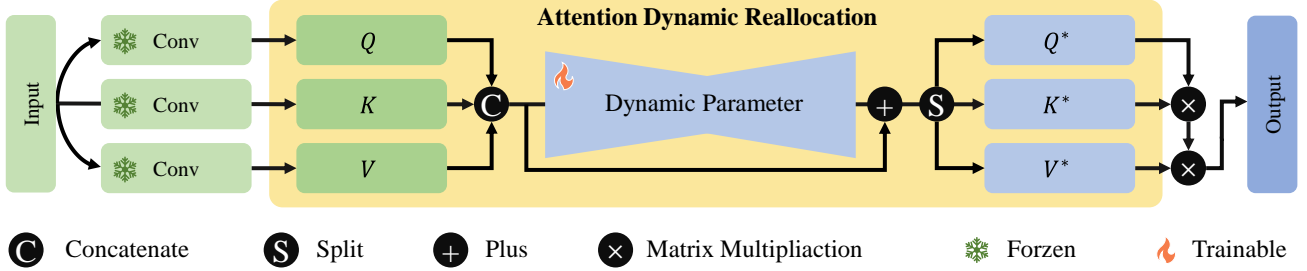


Figure 3. **Overview of Attention Dynamic Reallocation (ADR).** ADR leverages dynamic parameters to reallocate appropriate attention from the original attention.

It is reasonable for model redundancy to manifest as parameter harmfulness. After training, static parameters are consistently applied to all input images. This parameter sharing mechanism treats all images equally, disregarding differences in image content that cause the same parameters to have different effects on images with different degradation or textures [10, 59, 79]. As a result, the model tends to fit more common images while neglecting more challenging ones. Therefore, resetting some parameters can lead to decreasing performance for some images, while improving performance for others.

Uselessness. Model redundancy in dynamic parameters arises because the parameters are useless. Specifically, certain dynamic convolutions generate similar parameters for different images, rendering all candidate convolution parameters useless. Our experiments demonstrate this phenomenon, as the predicted parameters remain nearly identical when inputting various images. As shown in Figure 2 (b), dynamic parameters degrade to static parameters.

It is predictable for model redundancy to manifest as parameter uselessness. Without specific constraints, the dynamic convolution easily learns similar or relevant candidate convolutions [27], as even initialization [8] can lead to various correlations. Moreover, the direct weighting across the entire convolution dimension, rather than operating on a single parameter, exacerbates the degradation into static parameters. Consequently, some dynamic convolutions fail to contribute, yielding useless parameters.

3.2. Discussion

Discussion on differences. Firstly, model redundancy in dynamic parameters has not yet been explored. Secondly, the attributed reasons of model redundancy differ. Current researches attribute model redundancy to removable parameters for the whole dataset, which is semblance in our rethinking. We attribute model redundancy in static parameters to the harmful parameters at the individual image level. Lastly, the methods for mitigating model redundancy differ. While current research typically removes parameters to accelerate computation, we try to revise the error caused by

the harmful parameters.

Discussion on solutions. In summary, model redundancy manifests as parameter harmfulness in static parameters and parameter uselessness in dynamic parameters. Parameter harmfulness primarily stems from the parameter sharing mechanism and cannot be resolved simply by retraining. A feasible approach to mitigate harmfulness is adopting dynamic parameters to deal with the errors caused by harmfulness. However, dynamic parameters face the challenge of degrading into static parameters and becoming useless. Therefore, in this paper, we propose a parameter orthogonal generation (POG) technique and an attention dynamic reallocation (ADR) technique based on POG.

4. Method

4.1. Attention Dynamic Reallocation (ADR)

In this section, we propose attention dynamic reallocation (ADR). ADR reallocates appropriate attention from the original attention affected by parameter harmfulness, as illustrated in Figure 3.

In Section 3.2, we have discussed that dynamic parameters can mitigate parameter harmfulness. We further draw inspiration from the anterior cingulate cortex (ACC) to polish the practical details of our idea. The anterior cingulate cortex (ACC), located on the medial surface of the frontal lobes, is responsible for attention allocation, conflict monitoring, and error processing [3, 6, 7, 24]. Recent research has shown that attention allocation plays a role in error processing [36, 42, 57, 73]. Inspired by the human brain theory about attention allocation and error processing, we propose an attention dynamic reallocation (ADR) technique to address errors caused by parameter harmfulness.

ADR first concatenates the original Q , K , and V to derive the initial image attention denoted as $f_{in} \in \mathbb{R}^{D_h \times D_w \times D_c}$:

$$f_{in} = \text{Concat}(Q, K, V). \quad (1)$$

Here, D_h , D_w , and D_c represent the height, width, and

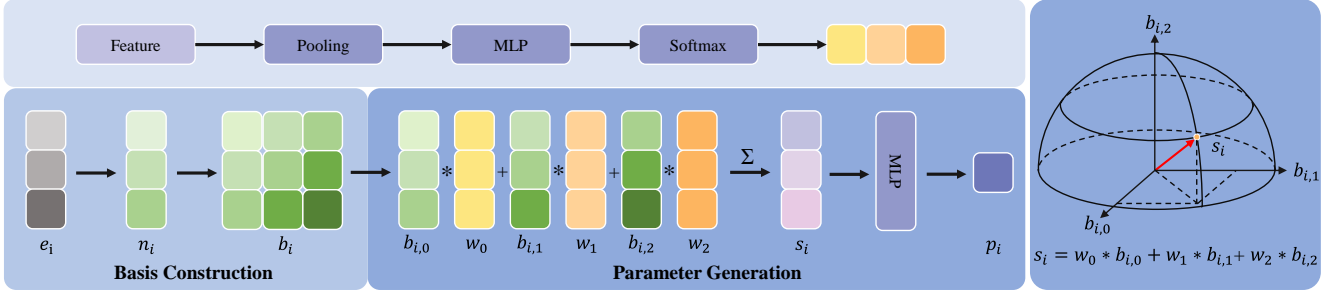


Figure 4. **Overview of Parameter Orthogonal Generation (POG)**. POG learns parameter embedding for each parameter, then constructs the orthogonal basis embeddings for the parameter, and finally generates specific parameters for the input image.

channel dimensions of the original image attention f_{in} , respectively.

Next, the original attention f_{in} is passed through a bottleneck structure [89] consisting of two convolutional layers to obtain the new attention f_{out} :

$$f_{out} = f_{in} + \mathcal{P}_{\theta_2} \circledast (\mathcal{P}_{\theta_1} \circledast f_{in}) \quad (2)$$

where $\mathcal{P}_{\theta_1} \in \mathbb{R}^{D_c \times D_m \times D_k^2}$ and $\mathcal{P}_{\theta_2} \in \mathbb{R}^{D_m \times D_c \times D_k^2}$ are the dynamically generated parameters. In addition, \circledast denotes the convolution operation, D_m denotes the channel dimension of the output of the first convolution, and D_k denotes the kernel size. The constraint $D_m < D_c$ leads to a squeeze-and-excitation effect on the channel dimension, forming a bottleneck structure. The bottleneck structure significantly reduces the parameters [89] while aiding in the excitation of important information, according to information bottleneck theory [60].

Finally, the output f_{out} is split to obtain new Q^* , K^* and V^* :

$$Q^*, K^*, V^* = \text{Split}(f_{out}). \quad (3)$$

The improved attention Q^* , K^* , and V^* reallocated by ADR provide the ability to mitigate parameter harmfulness while maintaining the overall architecture and processing flow of the original neural network model.

In summary, ADR draws insights from our observation to employ dynamic parameters and leverages inspiration from the human brain theory about attention allocation and error processing to dynamically reallocate attention, thereby effectively mitigating parameter harmfulness.

4.2. Parameter Orthogonal Generation (POG)

In this section, we introduce parameter orthogonal generation (POG), as illustrated in Figure 4.

Given an input image features f_{in} , POG generates specific parameters $\mathcal{P} \in \mathbb{R}^{C_{in} \times C_{out} \times D_k^2}$, where C_{in} , C_{out} , and D_k denote the numbers of input channels, output channels, and convolution kernel size, respectively. POG comprises

two primary steps: basis construction and parameter generation. Firstly, POG learns an embedding for each parameter and constructs orthogonal basis embeddings through the basis generation process. Subsequently, POG adaptively weights the basis embeddings to generate the specific embedding for the specific image and decodes specific parameters from the specific embedding.

Basis construction. Initially, POG learns parameter embeddings $\mathcal{E}_p \in \mathbb{R}^{N \times D_e \times 1}$ for the parameters P , where $N = C_{in} \times C_{out} \times D_k^2$ and D_e represents the embedding dimension. These embeddings, denoted as $\mathcal{E}_p = [e_1, e_2, \dots, e_N]$, correspond to each parameter e_i individually. After that, POG normalizes each column vector embedding e_i to obtain the normalized embeddings \mathcal{N}_p .

Next, POG constructs basis embeddings \mathcal{B}_p for parameters based on the normalized embeddings \mathcal{N}_p :

$$\mathcal{B}_p = I - 2\mathcal{N}_p\mathcal{N}_p^T. \quad (4)$$

where I is the identity matrix. Here, $\mathcal{B}_p \in \mathbb{R}^{N \times D_e \times D_e}$ consists of basis embeddings $b_i \in \mathbb{R}^{D_e \times D_e}$. Each basis embeddings b_i consist of one set of D_e orthogonal bases for each parameter e_i [25], where $b_{i,j} \in \mathbb{R}^{D_e \times 1}$, $1 \leq j \leq D_e$. Further theory guarantee regarding orthogonal bases is provided in the supplementary materials. The basis embeddings \mathcal{B}_p are fixed after training.

Parameter Generation. The specific parameters for each image are decoded from specific embeddings, which are constructed by adaptively weighting the basis embeddings.

The weights, derived from the input f_{in} , are obtained through the following process. Firstly, POG averages the spatial space of input f_{in} , then passes them through a 2-layer MLP [15], and finally applies Softmax to obtain the weights $\mathcal{W} = [w_1, w_2, \dots, w_{D_e}]^T \in \mathbb{R}^{D_e \times 1}$:

$$\mathcal{W} = \text{Softmax}(\mathcal{M}_{\theta_3}(\text{Pooling}(f_{in}))). \quad (5)$$

where \mathcal{M}_{θ_3} is a 2-layer MLP parameterized by θ_3 .

For each parameter, POG adaptively weights the basis embeddings to derive the specific embedding $S_p =$

Table 4. **Model redundancy among attention mechanism.** The DMR (\downarrow) metric is employed to detect model redundancy. A smaller DMR indicates a greater difference in the output results before and after resetting, reflecting lower model redundancy.

Methods	LOL-v1	LOL-v2-real	LOL-v2-syn
SNR-Net [77]	40.79	41.54	36.63
LLformer [66]	49.94	-	-
Retinexmamba [2]	42.86	40.76	42.64
Restormer [84]	48.94	47.34	49.53
Restormer+Ours	45.09	45.09	47.78
Retinexformer [5]	34.88	36.78	36.35
Retinexformer+Ours	29.03	33.42	34.86
CIDNet [14]	33.46	33.57	37.02
CIDNet+Ours	33.40	31.99	36.58

$[s_1, s_2, \dots, s_N] \in \mathbb{R}^{N \times D_e}$ specialized for the input f_{in} :

$$s_i = \sum_{j=1}^{D_e} w_j b_{i,j}. \quad (6)$$

This specific parameter embedding \mathcal{S}_p is then decoded using a 2-layer MLP \mathcal{M}_{θ_4} parameterized by θ_4 , extracting the final parameters \mathcal{P} :

$$\mathcal{P} = \mathcal{M}_{\theta_4}(\mathcal{S}_p), \quad (7)$$

The MLP \mathcal{M}_{θ_4} decodes a parameter from the corresponding specific embedding s_i . After reshaping the shape of parameters \mathcal{P} , the generation process is concluded.

In summary, POG learns orthogonal basis embeddings for single parameters, thus avoiding the correlation in embeddings and enable to operate at a single parameter level sensitively.

5. Experiments

5.1. Implementation Details

In the experiments, the channel dimension D_m is usually set to 32 and the embedding dim D_e is usually set to 64. As we aim to employ ADR to correct the harmfulness caused by preceding networks, we only employ ADR in the decoder of the Unet. In addition, the dynamic parameters are generated by the POG technique. More dataset details, implementation details, and additional visual results are provided in the supplementary materials.

5.2. Model Redundancy

Most existing studies focus on high-level tasks like object recognition and object detection, typically using FLOPs, accuracy rate and precision rate as the evaluation metric. However, these metrics are not suitable for LLIE. Here, we

Table 5. Comparison (PSNR \uparrow / DMR \downarrow) with methods in high-level vision tasks for mitigating model redundancy.

Methods	LOL-v1	LOL-v2-real	LOL-v2-syn
Restormer	20.91 / 48.94	20.79 / 47.34	24.06 / 49.53
PC-0.1 [20]	20.94 / 49.21	20.73 / 46.21	24.00 / 48.11
PC-0.2 [20]	20.83 / 50.00	20.99 / 45.63	23.82 / 48.19
PC-0.3 [20]	20.66 / 51.55	11.00 / —	12.63 / —
IENNP [21]	18.52 / 49.21	18.79 / 46.26	13.98 / —
FPGM [22]	18.07 / 48.89	20.66 / 46.07	13.31 / —
ZeroQ [4]	7.98 / —	9.75 / —	9.81 / —
Ours	21.88 / 45.09	21.49 / 45.09	24.56 / 47.78

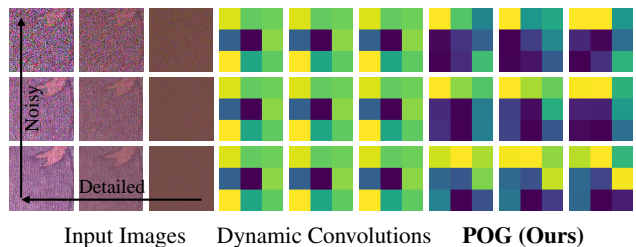


Figure 5. **Comparison of the generated dynamic parameters.** The dynamic parameters generated by POG for each row and column image exhibit gradual evolution processes, indicating that POG recognizes differences and understands similarities between these images. (The input low-light images have been brightened for better visibility.)

use the method in motivation experiments (Section 3.1) to detect model redundancy, denoted this metric as **DMR**.

Specifically, for each layer to be detected, we reset the parameters to random values and then calculate the differences between the images enhanced by the original model and those enhanced by the model with the reset parameters. Similar to PSNR, we use the logarithmic MSE to represent the differences, and the average logarithmic MSE across all layers is defined as DMR. For a given trained model F , let F_i represent the model where parameters of the i -th layer to be detected are reset. For a set of m test images x_j , the redundancy metric DMR is calculated as:

$$\text{DMR} = \sum_{i=1}^n \sum_{j=1}^m 10 \cdot \log_{10} \left(\frac{I_{\max}^2}{\text{MSE}(F(x_j), F_i(x_j))} \right), \quad (8)$$

where I_{\max} is the maximum pixel value of the image, typically 255 for 8-bit images.

A larger value of DMR suggests that even when the parameters are reset to random values, the model still produces results similar to a well-trained model with small differences, indicating high model redundancy. Conversely, a smaller DMR implies lower model redundancy.

We detect the model redundancy of the attention layers. As shown in Table 4, our techniques significantly reduce the

Table 6. Quantitative comparison (PSNR \uparrow and SSIM \uparrow) on paired datasets. Our techniques improve LLIE performance.

Methods	Publication	FLOPs (G)	LOL-v1 [74]		LOL-v2-real [80]		LOL-v2-syn [80]	
			PSNR \uparrow	SSIM \uparrow	PSNR \uparrow	SSIM \uparrow	PSNR \uparrow	SSIM \uparrow
RetinexNet [74]	BMVC 2018	587.47	16.77	0.560	15.47	0.567	17.13	0.798
KinD [87]	MM 2019	34.99	20.86	0.790	14.74	0.641	13.29	0.578
Enlightengan [32]	TIP 2021	61.01	17.48	0.650	18.23	0.617	16.57	0.734
RUAS [87]	CVPR 2021	0.83	18.23	0.720	18.37	0.723	16.55	0.652
SNRNet [77]	CVPR2022	26.35	24.61	0.842	21.48	0.849	24.14	0.928
LLformer [66]	AAAI 2023	22.52	23.65	0.816	20.06	0.792	24.04	0.909
GSAD [26]	NeurIPS 2023	-	22.88	0.849	20.19	0.847	24.22	0.927
QuadPrior [68]	CVPR 2024	-	20.31	0.808	-	-	-	-
RSFNet [56]	CVPR 2024	-	19.39	0.755	19.27	0.738	-	-
Retinexmamba [2]	Arxiv 2024	42.82	24.03	0.827	22.45	0.844	25.89	0.935
Restormer [84]	CVPR 2022	144.25	20.91	0.788	20.79	0.816	24.06	0.919
Restormer+Ours	-	145.99	21.88	0.797	21.49	0.813	24.56	0.926
Retinexformer [5]	ICCV 2023	15.85	25.16	0.845	22.80	0.840	25.67	0.930
Retinexformer+Ours	-	16.56	25.29	0.845	22.87	0.842	25.78	0.930
CIDNet [14]	Arxiv 2024	7.57	23.81	0.857	23.90	0.866	25.71	0.942
CIDNet+Ours	-	8.17	23.97	0.859	24.21	0.866	26.02	0.942

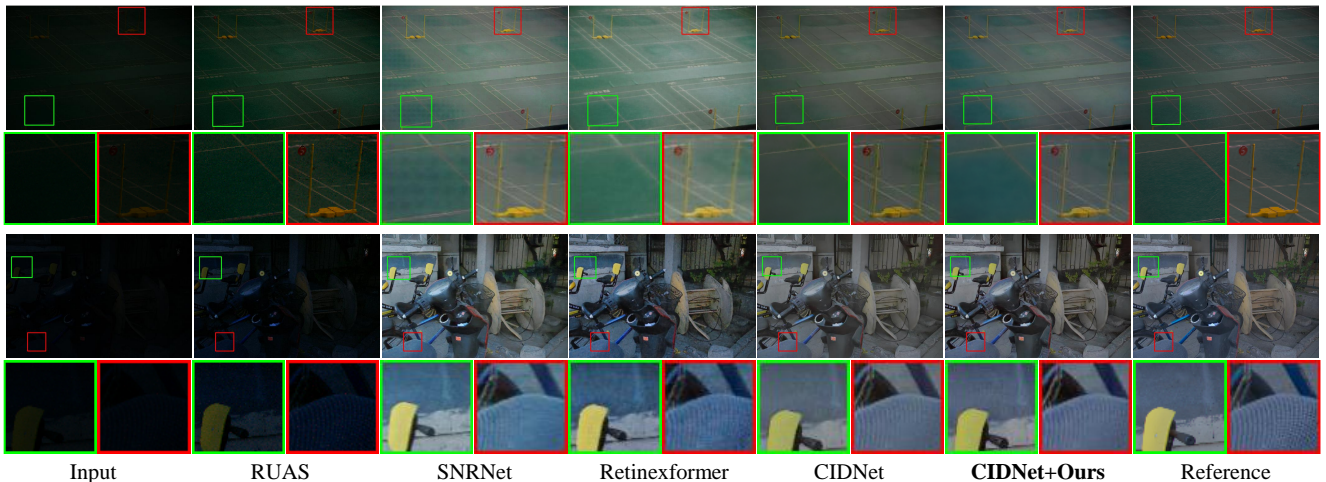


Figure 6. Qualitative comparison on LOL-v1 [74] and LOL-v2 [80] datasets.

DMR, effectively decreasing model redundancy. Furthermore, as illustrated in Figure 5, POG can accurately generate unique parameters for each image, while the dynamic convolution degrades to using fixed parameters.

We also compare methods that are widely recognized in other tasks for mitigating model redundancy. However, these methods not only can not effectively reduce DMR, but also reduce performance as shown in Table 5. On the LOL-v2-synthetic [80] dataset, many methods (IENNP [21] and FPGM [22]) reduce 10% channels, but the LLIE performance collapses directly. This phenomenon may result from the shift in the parameter distribution [50], leading to color distortion in the output images. Such distortion may

be acceptable for high-level tasks but is unacceptable for LLIE, which aims to enhance color and illumination.

5.3. Low-Light Image Enhancement

For paired datasets, we conduct experiments following previous research [2, 14], evaluating our techniques on the popular LOL-v1 [74], LOL-v2-real [80], and LOL-v2-synthetic [80] datasets. Table 6 presents a quantitative comparison of various methods. Our techniques achieve varying degrees of PSNR improvement based on different model redundancy. Specifically, our techniques achieve a PSNR improvement of about 1 dB compared to the Restormer method and over 0.3 dB compared to the CIDNet method. Figure 6 illustrates the visual results for the LOL datasets,

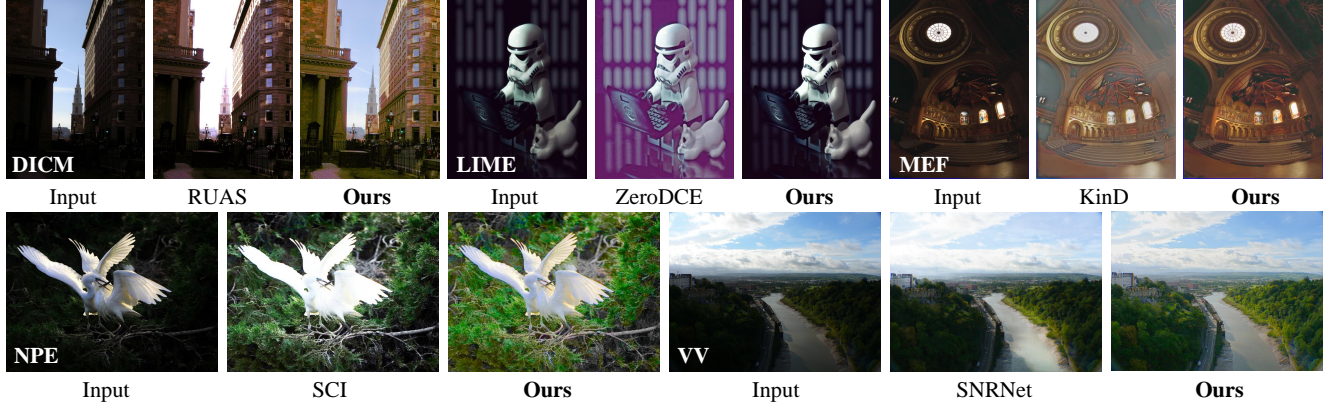


Figure 7. Qualitative comparison on DICM [37], LIME [18], MEF [46], NPE [65], and VV [63] datasets.

Table 7. Ablation study on the ADR technique and POG technique.

Methods	PSNR \uparrow	FLOPs (G) \downarrow
Restormer	20.91	144.25
Restormer + static conv	21.18	145.69
Restormer + ADR	21.60	145.87
Restormer + ADR + POG	21.88	145.99

Table 8. Ablation study on hyperparameters of ADR.

Methods	PSNR \uparrow	FLOPs (G) \downarrow
Restormer	20.91	144.25
$D_m = 4$	21.88	145.99
$D_m = 8$	21.92	147.55
$D_m = 16$	21.77	150.67

Table 9. Ablation study on hyperparameters of POG.

Methods	PSNR \uparrow	FLOPs (G) \downarrow
Restormer	20.91	144.25
$D_e = 16$	21.53	145.88
$D_e = 32$	21.86	145.90
$D_e = 64$	21.88	145.99

Table 10. Quantitative comparison (NIQE \downarrow) on unpaired datasets.

Methods	DICM	LIME	MEF	NPE	VV	Mean
KinD [87]	5.15	5.03	5.47	4.98	4.30	4.99
ZeroDCE [39]	4.58	5.82	4.93	4.53	4.81	4.93
RUAS [55]	5.21	4.26	3.83	5.53	4.29	4.62
LLFlow [69]	4.06	4.59	4.70	4.67	4.04	4.41
SNRNet [77]	4.71	5.74	4.18	4.32	9.87	5.76
PairLIE [16]	4.03	4.58	4.06	4.18	3.57	4.08
GLARE [90]	3.61	4.52	3.66	4.19	-	4.10
Restormer [84]	3.49	4.31	3.71	3.97	2.93	3.68
Restormer+Ours	3.42	4.25	3.66	3.96	2.81	3.62
Retinexformer [5]	3.85	4.31	3.67	3.76	3.09	3.74
Retinexformer+Ours	3.51	4.00	3.62	3.92	3.00	3.61
CIDNet [14]	3.79	4.13	3.56	3.74	3.21	3.67
CIDNet+Ours	3.50	3.41	3.08	4.23	3.19	3.48

demonstrating our techniques learn accurate color.

For unpaired datasets, our techniques also achieve effective improvement, as shown in Table 10 and Figure 7. More experiments and visual results are provided in the supplementary materials.

5.4. Ablation Study

In this section, we conduct a comprehensive ablation study of our techniques.

Component Analysis. In the “Restormer+ADR” setting, the parameters are generated by traditional dynamic convolutions and in “Restormer+ADR+POG”, the parameters are generated by POG. Incorporating only static convolutions into Restormer results in a slight improvement as demonstrated in Table 7. Both our ADR and POG improve the performance, highlighting the effectiveness of each technique.

Hyperparameter Analysis. We further investigate the impact of different hyperparameter settings, as shown in Table 8 and Table 9. Increasing the dimension D_m leads to an increase in FLOPs but slightly improves the PSNR. This result aligns with the design goal of employing the bottleneck structure in ADR. In addition, the computation is more sensitive to the dimension D_m than the embedding dim D_e . Thus, for bigger methods (such as Restormer), we set smaller dimensions D_m (usually $D_m = 4$) to accelerate computation.

6. Conclusion

In this paper, we rethink the model redundancy of LLIE, which establishes the foundation to mitigate model redundancy while improving LLIE performance. We identify model redundancy manifesting as parameter harmfulness and parameter uselessness and propose ADR and POG to tackle these issues, respectively. In the future, we will employ the model redundancy rethinking to guide the effective architecture design.

References

- [1] Nima Aghli and Eraldo Ribeiro. Combining weight pruning and knowledge distillation for cnn compression. *Proceedings of the IEEE/CVF Conference on Computer Vision and Pattern Recognition (CVPR)*, pages 3191–3198, 2021. [1](#), [2](#)
- [2] Jiesong Bai, Yuhao Yin, and Qiyuan He. Retinexmamba: Retinex-based mamba for low-light image enhancement. *arXiv preprint arXiv:2405.03349*, pages 1–15, 2024. [1](#), [2](#), [6](#), [7](#)
- [3] Matthew M Botvinick, Todd S Braver, Deanna M Barch, Cameron S Carter, and Jonathan D Cohen. Conflict monitoring and cognitive control. *Psychological Review*, page 624, 2001. [4](#)
- [4] Yaohui Cai, Zhewei Yao, Zhen Dong, Amir Gholami, Michael W Mahoney, and Kurt Keutzer. Zeroq: A novel zero shot quantization framework. *Proceedings of the IEEE/CVF Conference on Computer Vision and Pattern Recognition (CVPR)*, pages 13169–13178, 2020. [1](#), [2](#), [6](#)
- [5] Yuanhao Cai, Hao Bian, Jing Lin, Haoqian Wang, Radu Timofte, and Yulun Zhang. Retinexformer: One-stage retinex-based transformer for low-light image enhancement. *Proceedings of the IEEE/CVF International Conference on Computer Vision (ICCV)*, pages 12504–12513, 2023. [1](#), [2](#), [6](#), [7](#), [8](#)
- [6] Cameron S Carter, Todd S Braver, Deanna M Barch, Matthew M Botvinick, Douglas Noll, and Jonathan D Cohen. Anterior cingulate cortex, error detection, and the online monitoring of performance. *Science*, pages 747–749, 1998. [2](#), [4](#)
- [7] Cameron S Carter, Matthew M Botvinick, and Jonathan D Cohen. The contribution of the anterior cingulate cortex to executive processes in cognition. *Reviews in the Neurosciences*, pages 49–58, 1999. [2](#), [4](#)
- [8] Stephen Casper, Xavier Boix, Vanessa D’Amario, Christopher Rodriguez, Ling Guo, Kasper Vinken, and Gabriel Kreiman. Removable and/or repeated units emerge in overparametrized deep neural networks. *arXiv preprint arXiv:1912.04783*, pages 1–9, 2019. [1](#), [4](#)
- [9] Edward A Catchpole and Byron JT Morgan. Detecting parameter redundancy. *Biometrika*, pages 187–196, 1997. [2](#)
- [10] Yinpeng Chen, Xiyang Dai, Mengchen Liu, Dongdong Chen, Lu Yuan, and Zicheng Liu. Dynamic convolution: Attention over convolution kernels. *Proceedings of the IEEE/CVF Conference on Computer Vision and Pattern Recognition (CVPR)*, pages 11030–11039, 2020. [3](#), [4](#)
- [11] Hengda Cheng and XJ Shi. A simple and effective histogram equalization approach to image enhancement. *Digital Signal Processing*, pages 158–170, 2004. [2](#)
- [12] Matthew Dutson, Yin Li, and Mohit Gupta. Eventful transformers: Leveraging temporal redundancy in vision transformers. *Proceedings of the IEEE/CVF International Conference on Computer Vision (ICCV)*, pages 16911–16923, 2023. [1](#), [2](#)
- [13] Gongfan Fang, Xinyin Ma, Mingli Song, Michael Bi Mi, and Xinchao Wang. Depgraph: Towards any structural pruning. *Proceedings of the IEEE/CVF Conference on Computer Vision and Pattern Recognition (CVPR)*, pages 16091–16101, 2023. [2](#)
- [14] Yixu Feng, Cheng Zhang, Pei Wang, Peng Wu, Qingsen Yan, and Yanning Zhang. You only need one color space: An efficient network for low-light image enhancement. *arXiv preprint arXiv:2402.05809*, pages 1–9, 2024. [6](#), [7](#), [8](#)
- [15] Rosenblatt Frank. The perceptron: A probabilistic model for information storage and organization in the brain. *Psychological Review*, page 386, 1958. [5](#)
- [16] Zhenqi Fu, Yan Yang, Xiaotong Tu, Yue Huang, Xinghao Ding, and Kai-Kuang Ma. Learning a simple low-light image enhancer from paired low-light instances. *Proceedings of the IEEE/CVF Conference on Computer Vision and Pattern Recognition (CVPR)*, pages 22252–22261, 2023. [8](#)
- [17] Hang Guo, Jinmin Li, Tao Dai, Zhihao Ouyang, Xudong Ren, and Shu-Tao Xia. Mambair: A simple baseline for image restoration with state-space model. *arXiv preprint arXiv:2402.15648*, pages 1–19, 2024. [1](#), [2](#)
- [18] Xiaojie Guo, Yu Li, and Haibin Ling. Lime: Low-light image enhancement via illumination map estimation. *IEEE Transactions on Image Processing (TIP)*, pages 982–993, 2016. [2](#), [8](#)
- [19] Song Han, Huizi Mao, and William J Dally. Deep compression: Compressing deep neural networks with pruning, trained quantization and huffman coding. *arXiv preprint arXiv:1510.00149*, pages 1–13, 2015. [1](#), [2](#)
- [20] Song Han, Jeff Pool, John Tran, and William Dally. Learning both weights and connections for efficient neural network. *Advances in Neural Information Processing Systems*, pages 1–9, 2015. [1](#), [2](#), [6](#)
- [21] Li Hao, Kadav Asim, Durdanovic Igor, Samet Hanan, and Graf HansPeter. Importance estimation for neural network pruning. *International Conference on Learning Representations (ICLR)*, pages 1–12, 2017. [6](#), [7](#)
- [22] Yang He, Ping Liu, Ziwei Wang, Zhilan Hu, and Yi Yang. Filter pruning via geometric median for deep convolutional neural networks acceleration. *Proceedings of the IEEE Conference on Computer Vision and Pattern Recognition (CVPR)*, pages 4340–4349, 2019. [1](#), [2](#), [6](#), [7](#)
- [23] Geoffrey Hinton, Oriol Vinyals, and Jeff Dean. Distilling the knowledge in a neural network. *arXiv preprint arXiv:1503.02531*, pages 1–9, 2015. [1](#), [2](#)
- [24] Clay B Holroyd, Sander Nieuwenhuis, Rogier B Mars, and Michael GH Coles. Anterior cingulate cortex, selection for action, and error processing. *Cognitive neuroscience of attention*, pages 219–231, 2004. [4](#)
- [25] Roger A Horn and Charles R Johnson. *Matrix Analysis*. Cambridge University Press, 1990. [2](#), [5](#)
- [26] Jinhui Hou, Zhiyu Zhu, Junhui Hou, Hui Liu, Huanqiang Zeng, and Hui Yuan. Global structure-aware diffusion process for low-light image enhancement. *Advances in Neural Information Processing Systems*, pages 79734–79747, 2024. [2](#), [7](#)
- [27] El Houssaine Hssayni, Nour-Eddine Joudar, and Mohamed Ettaouil. Krr-cnn: kernels redundancy reduction in convolutional neural networks. *Neural Computing and Applications*, pages 2443–2454, 2022. [2](#), [4](#)

- [28] ShihChia Huang, FanChieh Cheng, and YiSheng Chiu. Efficient contrast enhancement using adaptive gamma correction with weighting distribution. *IEEE Transactions on Image Processing (TIP)*, pages 1032–1041, 2012. 2
- [29] Max Jaderberg, Andrea Vedaldi, and Andrew Zisserman. Speeding up convolutional neural networks with low rank expansions. *arXiv preprint arXiv:1405.3866*, pages 1–12, 2014. 2
- [30] Hai Jiang, Ao Luo, Haoqiang Fan, Songchen Han, and Shuaicheng Liu. Low-light image enhancement with wavelet-based diffusion models. *ACM Transactions on Graphics (TOG)*, pages 1–14, 2023. 1, 2
- [31] Jingjing Jiang and Nanning Zheng. Mixphm: redundancy-aware parameter-efficient tuning for low-resource visual question answering. *Proceedings of the IEEE/CVF Conference on Computer Vision and Pattern Recognition (CVPR)*, pages 24203–24213, 2023. 2
- [32] Yifan Jiang, Xinyu Gong, Ding Liu, Yu Cheng, Chen Fang, Xiaohui Shen, Jianchao Yang, Pan Zhou, and Zhangyang Wang. Enlightengan: Deep light enhancement without paired supervision. *IEEE Transactions on Image Processing (TIP)*, pages 2340–2349, 2021. 1, 2, 7
- [33] Shibo Jie, Haoqing Wang, and Zhi-Hong Deng. Revisiting the parameter efficiency of adapters from the perspective of precision redundancy. *Proceedings of the IEEE/CVF International Conference on Computer Vision (CVPR)*, pages 17217–17226, 2023. 2
- [34] Daniel J Jobson, Zia-ur Rahman, and Glenn A Woodell. A multiscale retinex for bridging the gap between color images and the human observation of scenes. *IEEE Transactions on Image Processing (TIP)*, pages 965–976, 1997. 2
- [35] Daniel J Jobson, Zia-ur Rahman, and Glenn A Woodell. Properties and performance of a center/surround retinex. *IEEE Transactions on Image Processing (TIP)*, pages 451–462, 1997. 2
- [36] Joseph A King, Franziska M Korb, D Yves von Cramon, and Markus Ullsperger. Post-error behavioral adjustments are facilitated by activation and suppression of task-relevant and task-irrelevant information processing. *Journal of Neuroscience*, pages 12759–12769, 2010. 4
- [37] Chulwoo Lee, Chul Lee, and Chang-Su Kim. Contrast enhancement based on layered difference representation of 2d histograms. *IEEE Transactions on Image Processing (TIP)*, pages 5372–5384, 2013. 8
- [38] Chongyi Li, Chunle Guo, Linghao Han, Jun Jiang, Mingming Cheng, Jinwei Gu, and Chen Change Loy. Low-light image and video enhancement using deep learning: A survey. *IEEE Transactions on Pattern Analysis and Machine Intelligence (TPAMI)*, pages 9396–9416, 2022. 1
- [39] Chongyi Li, Chunle Guo, and Chen Change Loy. Learning to enhance low-light image via zero-reference deep curve estimation. *IEEE Transactions on Pattern Analysis and Machine Intelligence (TPAMI)*, pages 4225–4238, 2022. 2, 8
- [40] Jiafeng Li, Ying Wen, and Lianghua He. Sconv: Spatial and channel reconstruction convolution for feature redundancy. *Proceedings of the IEEE/CVF Conference on Computer Vision and Pattern Recognition (CVPR)*, pages 6153–6162, 2023. 2
- [41] Mading Li, Jiaying Liu, Wenhan Yang, Xiaoyan Sun, and Zongming Guo. Structure-revealing low-light image enhancement via robust retinex model. *IEEE Transactions on Image Processing (TIP)*, pages 2828–2841, 2018. 2
- [42] Qing Li, Jing Wang, Zhifang Li, and Antao Chen. Decoding the specificity of post-error adjustments using eeg-based multivariate pattern analysis. *Journal of Neuroscience*, pages 6800–6809, 2022. 2, 4
- [43] Jinxiu Liang, Jingwen Wang, Yuhui Quan, Tianyi Chen, Jiaying Liu, Haibin Ling, and Yong Xu. Recurrent exposure generation for low-light face detection. *IEEE Transactions on Multimedia*, pages 1609–1621, 2021. 1, 2
- [44] Jiaying Liu, DeJia Xu, Wenhan Yang, Minhao Fan, and Haofeng Huang. Benchmarking low-light image enhancement and beyond. *International Journal of Computer Vision*, pages 1153–1184, 2021. 1, 2
- [45] Zhuang Liu, Jianguo Li, Zhiqiang Shen, Gao Huang, Shoumeng Yan, and Changshui Zhang. Learning efficient convolutional networks through network slimming. *Proceedings of the IEEE/CVF International Conference on Computer Vision (ICCV)*, pages 2736–2744, 2017. 1, 2
- [46] Kede Ma, Kai Zeng, and Zhou Wang. Perceptual quality assessment for multi-exposure image fusion. *IEEE Transactions on Image Processing (TIP)*, pages 3345–3356, 2015. 8
- [47] Carl D Meyer. *Matrix analysis and applied linear algebra*, 2000. 2
- [48] Pavlo Molchanov, Arun Mallya, Stephen Tyree, Iuri Frosio, and Jan Kautz. Importance estimation for neural network pruning. *Proceedings of the IEEE/CVF Conference on Computer Vision and Pattern Recognition (CVPR)*, pages 11264–11272, 2019. 2
- [49] Sean Moran, Pierre Marza, Steven McDonagh, Sarah Parisot, and Gregory Slabaugh. Deeplpf: Deep local parametric filters for image enhancement. *Proceedings of the IEEE/CVF Conference on Computer Vision and Pattern Recognition (CVPR)*, pages 12826–12835, 2020. 2
- [50] Markus Nagel, Mart van Baalen, Tijmen Blankevoort, and Max Welling. Data-free quantization through weight equalization and bias correction. *Proceedings of the IEEE/CVF International Conference on Computer Vision (ICCV)*, pages 1325–1334, 2019. 1, 2, 7
- [51] Chen Hee Ooi and Nor Ashidi Mat Isa. Quadrants dynamic histogram equalization for contrast enhancement. *IEEE Transactions on Consumer Electronics*, pages 2552–2559, 2010. 2
- [52] Etta D Pisano, Shuquan Zong, Bradley M Hemminger, Marla DeLuca, R Eugene Johnston, Keith Muller, M Patricia Braeuning, and Stephen M Pizer. Contrast limited adaptive histogram equalization image processing to improve the detection of simulated spiculations in dense mammograms. *Journal of Digital imaging*, pages 193–200, 1998. 2
- [53] Stephen M Pizer, E Philip Amburn, John D Austin, Robert Cromartie, Ari Geselowitz, Trey Greer, Bart ter Haar Romeny, John B Zimmerman, and Karel Zuiderveld. Adaptive histogram equalization and its variations. *Computer Vision, Graphics, and Image Processing*, pages 355–368, 1987. 2

- [54] Roberto Rigamonti, Amos Sironi, Vincent Lepetit, and Pascal Fua. Learning separable filters. *Proceedings of the IEEE/CVF Conference on Computer Vision and Pattern Recognition (CVPR)*, pages 2754–2761, 2013. 1, 2
- [55] Liu Risheng, Ma Long, Zhang Jiaao, Fan Xin, and Luo Zhongxuan. Retinex-inspired unrolling with cooperative prior architecture search for low-light image enhancement. *Proceedings of the IEEE/CVF Conference on Computer Vision and Pattern Recognition (CVPR)*, 2021. 8
- [56] Saurabh Saini and P. J. Narayanan. Specularity factorization for low light enhancement. *Proceedings of the IEEE/CVF Conference on Computer Vision and Pattern Recognition (CVPR)*, pages 1–12, 2024. 7
- [57] Hans S Schroder, Megan E Fisher, Yanli Lin, Sharon L Lo, Judith H Danovitch, and Jason S Moser. Neural evidence for enhanced attention to mistakes among school-aged children with a growth mindset. *Developmental Cognitive Neuroscience*, pages 42–50, 2017. 2, 4
- [58] Aashish Sharma and Robby T Tan. Nighttime visibility enhancement by increasing the dynamic range and suppression of light effects. *Proceedings of the IEEE/CVF Conference on Computer Vision and Pattern Recognition (CVPR)*, pages 11977–11986, 2021. 2
- [59] Hao Shen, Zhong-Qiu Zhao, and Wandi Zhang. Adaptive dynamic filtering network for image denoising. *Proceedings of the AAAI Conference on Artificial Intelligence (AAAI)*, pages 2227–2235, 2023. 4
- [60] Naftali Tishby and Noga Zaslavsky. Deep learning and the information bottleneck principle. *2015 IEEE Information Theory Workshop*, pages 1–5, 2015. 5
- [61] Ashish Vaswani, Noam Shazeer, Niki Parmar, Jakob Uszkoreit, Llion Jones, Aidan N Gomez, Łukasz Kaiser, and Illia Polosukhin. Attention is all you need. *Advances in Neural Information Processing Systems*, pages 1–11, 2017. 1
- [62] Elena Voita, David Talbot, Fedor Moiseev, Rico Sennrich, and Ivan Titov. Analyzing multi-head self-attention: Specialized heads do the heavy lifting, the rest can be pruned. *Proceedings of the 57th Annual Meeting of the Association for Computational Linguistics*, pages 5797–5808, 2019. 1
- [63] Vassilios Vonikakis, Rigas Kouskouridas, and Antonios Gasteratos. On the evaluation of illumination compensation algorithms. *Multimedia Tools and Applications*, pages 1–21, 2018. 8
- [64] Ruixing Wang, Qing Zhang, Chiwing Fu, Xiaoyong Shen, Weishi Zheng, and Jiaya Jia. Underexposed photo enhancement using deep illumination estimation. *Proceedings of the IEEE/CVF Conference on Computer Vision and Pattern Recognition (CVPR)*, pages 6849–6857, 2019. 2
- [65] Shuhang Wang, Jin Zheng, Hai-Miao Hu, and Bo Li. Naturalness preserved enhancement algorithm for non-uniform illumination images. *IEEE Transactions on Image Processing (TIP)*, pages 3538–3548, 2013. 2, 8
- [66] Tao Wang, Kaihao Zhang, Tianrun Shen, Wenhan Luo, Bjorn Stenger, and Tong Lu. Ultra-high-definition low-light image enhancement: A benchmark and transformer-based method. *Proceedings of the AAAI Conference on Artificial Intelligence (AAAI)*, pages 2654–2662, 2023. 2, 6, 7
- [67] Wenjing Wang, Chen Wei, Wenhan Yang, and Jiaying Liu. Gladnet: Low-light enhancement network with global awareness. *IEEE International Conference on Automatic Face and Gesture Recognition*, pages 751–755, 2018. 2
- [68] Wenjing Wang, Huan Yang, Jianlong Fu, and Jiaying Liu. Zero-reference low-light enhancement via physical quadruple priors. *Proceedings of the IEEE/CVF Conference on Computer Vision and Pattern Recognition (CVPR)*, pages 26057–26066, 2024. 7
- [69] Yufei Wang, Renjie Wan, Wenhan Yang, Haoliang Li, Lap-Pui Chau, and Alex Kot. Low-light image enhancement with normalizing flow. *Proceedings of the AAAI Conference on Artificial Intelligence (AAAI)*, pages 2604–2612, 2022. 8
- [70] Yinglong Wang, Zhen Liu, Jianzhuang Liu, Songcen Xu, and Shuaicheng Liu. Low-light image enhancement with illumination-aware gamma correction and complete image modelling network. *Proceedings of the IEEE/CVF International Conference on Computer Vision (ICCV)*, pages 13128–13137, 2023. 2
- [71] Zhiguo Wang, Zhihu Liang, and Chunliang Liu. A real-time image processor with combining dynamic contrast ratio enhancement and inverse gamma correction for pdp. *Displays*, pages 133–139, 2009. 2
- [72] Zi Wang, Chengcheng Li, and Xiangyang Wang. Convolutional neural network pruning with structural redundancy reduction. *Proceedings of the IEEE/CVF Conference on Computer Vision and Pattern Recognition (CVPR)*, pages 14913–14922, 2021. 2
- [73] Xiaoru Wanyan, Damin Zhuang, Hengyang Wei, and Jianshuang Song. Pilot attention allocation model based on fuzzy theory. *Computers & Mathematics with Applications*, pages 2727–2735, 2011. 4
- [74] Chen Wei, Wenjing Wang, Wenhan Yang, and Jiaying Liu. Deep retinex decomposition for low-light enhancement. *British Machine Vision Conference (BMVC)*, pages 1–12, 2018. 1, 2, 7
- [75] Jiangwei Weng, Zhiqiang Yan, Ying Tai, Jianjun Qian, Jian Yang, and Jun Li. Mamballie: Implicit retinex-aware low light enhancement with global-then-local state space. *arXiv preprint arXiv:2405.16105*, pages 1–12, 2024. 2
- [76] Bin Xia, Yulun Zhang, Shiyin Wang, Yitong Wang, Xinglong Wu, Yapeng Tian, Wenming Yang, and Luc Van Gool. Diffir: Efficient diffusion model for image restoration. *Proceedings of the IEEE/CVF Conference on Computer Vision and Pattern Recognition (CVPR)*, pages 13095–13105, 2023. 1
- [77] Xiaogang Xu, Ruixing Wang, Chiwing Fu, and Jiaya Jia. Snr-aware low-light image enhancement. *Proceedings of the IEEE/CVF Conference on Computer Vision and Pattern Recognition (CVPR)*, pages 17714–17724, 2022. 2, 6, 7, 8
- [78] Yusyuan Xu, Shouyao Roy Tseng, Yu Tseng, Hsienkai Kuo, and Yi-Min Tsai. Unified dynamic convolutional network for super-resolution with variational degradations. *Proceedings of the IEEE/CVF Conference on Computer Vision and Pattern Recognition (CVPR)*, pages 12496–12505, 2020. 1
- [79] Brandon Yang, Gabriel Bender, Quoc V Le, and Jiquan Ngiam. Condconv: Conditionally parameterized convolu-

- tions for efficient inference. *Advances in Neural Information Processing Systems*, pages 1–11, 2019. 2, 4
- [80] Wenhan Yang, Wenjing Wang, Haofeng Huang, Shiqi Wang, and Jiaying Liu. Sparse gradient regularized deep retinex network for robust low-light image enhancement. *IEEE Transactions on Image Processing (TIP)*, pages 2072–2086, 2021. 7
- [81] Man Yao, Jiakui Hu, Guangshe Zhao, Yaoyuan Wang, Ziyang Zhang, Bo Xu, and Guoqi Li. Inherent redundancy in spiking neural networks. *Proceedings of the IEEE/CVF International Conference on Computer Vision (ICCV)*, pages 16924–16934, 2023. 2
- [82] Xunpeng Yi, Han Xu, Hao Zhang, Linfeng Tang, and Jiayi Ma. Diff-retinex: Rethinking low-light image enhancement with a generative diffusion model. *Proceedings of the IEEE/CVF International Conference on Computer Vision (ICCV)*, pages 12302–12311, 2023. 2
- [83] Syed Waqas Zamir, Aditya Arora, Salman Khan, Munawar Hayat, Fahad Shahbaz Khan, MingHsuan Yang, and Ling Shao. Learning enriched features for fast image restoration and enhancement. *IEEE Transactions on Pattern Analysis and Machine Intelligence (TPAMI)*, pages 1934–1948, 2022. 2
- [84] Syed Waqas Zamir, Aditya Arora, Salman Khan, Munawar Hayat, Fahad Shahbaz Khan, and Ming-Hsuan Yang. Restormer: Efficient transformer for high-resolution image restoration. *Proceedings of the IEEE/CVF Conference on Computer Vision and Pattern Recognition (CVPR)*, pages 5728–5739, 2022. 1, 2, 3, 6, 7, 8
- [85] Kai Zhang, Wangmeng Zuo, and Lei Zhang. Learning a single convolutional super-resolution network for multiple degradations. *Proceedings of the IEEE/CVF Conference on Computer Vision and Pattern Recognition (CVPR)*, pages 3262–3271, 2018. 1
- [86] Xuanqi Zhang, Haijin Zeng, Jinwang Pan, Qiangqiang Shen, and Yongyong Chen. Llemamba: Low-light enhancement via relighting-guided mamba with deep unfolding network. *arXiv preprint arXiv:2406.01028*, pages 1–12, 2024. 2
- [87] Yonghua Zhang, Jiawan Zhang, and Xiaojie Guo. Kindling the darkness: A practical low-light image enhancer. *Proceedings of the ACM International Conference on MultiMedia*, pages 1632–1640, 2019. 2, 7, 8
- [88] Yonghua Zhang, Xiaojie Guo, Jiayi Ma, Wei Liu, and Jiawan Zhang. Beyond brightening low-light images. *International Journal of Computer Vision*, pages 1013–1037, 2021. 2
- [89] Daquan Zhou, Qibin Hou, Yunpeng Chen, Jiashi Feng, and Shuicheng Yan. Rethinking bottleneck structure for efficient mobile network design. *European Conference on Computer Vision (ECCV)*, pages 680–697, 2020. 5
- [90] Han Zhou, Wei Dong, Xiaohong Liu, Shuaicheng Liu, Xiongkuo Min, Guangtao Zhai, and Jun Chen. Glare: Low light image enhancement via generative latent feature based codebook retrieval. In *Proceedings of the European Conference on Computer Vision (ECCV)*, pages 1–19, 2024. 2, 8